Environmental Science Processes & Impacts

Raw Material Recovery from Hydraulic Fracturing Residual Solid Waste with Implications for Sustainability and Radioactive Waste Disposal

Journal:	*Environmental Science: Processes & Impacts*
Manuscript ID	EM-ART-06-2018-000248.R1
Article Type:	Paper
Date Submitted by the Author:	21-Aug-2018

Complete List of Authors:	Ajemigbitse, Moses; The Pennsylvania State University, Civil and Environmental Engineering Cannon, Fred; The Pennsylvania State University, Civil and Environmental Engineering Klima, Mark; The Pennsylvania State University, John and Willie Leone Family Department of Energy and Mineral Engineering Furness, James; Furness-Newburge, Inc. Wunz, Chris; HydroRecovery, LP Warner, Nathaniel; The Pennsylvania State University, Civil and Environmental Engineering

Department of Civil and Environmental Engineering
College of Engineering
The Pennsylvania State University
212 Sackett Building
University Park, PA 16802-1408

814-863-3084
Fax: 814-863-7304
www.cee.psu.edu

Environmental Significance Statement for "Raw Material Recovery from Hydraulic Fracturing Residual Solid Waste with Implications for Sustainability and Radioactive Waste Disposal" by Moses A. Ajemigbitse, Fred S. Cannon, Mark Klima, James C. Furness, Chris Wunz, and Nathaniel R. Warner.

Energy production by hydraulic fracturing consumes significant volumes of raw materials (sand, clay and water). Conventionally, the solid wastes from this process are disposed to landfills despite containing recoverable raw materials. In addition, natural radioactivity from the formation returns to the surface with the flow of oil or gas and co-produced water. This radioactivity can often become concentrated in the solid waste. In a bid to make hydraulic fracturing more sustainable, we explored a treatment process of this solid waste that could reclaim raw materials; reduce waste volumes; and a reduce/mitigate radioactivity in the environment.

Raw Material Recovery from Hydraulic Fracturing Residual Solid Waste with Implications for Sustainability and Radioactive Waste Disposal

Moses A. Ajemigbitse, [a]* Fred S. Cannon, [a] Mark Klima, [b] James C. Furness, [c] Chris Wunz, [d] and Nathaniel R. Warner [a]

Abstract

Unconventional oil and gas residual solid wastes are generally disposed in municipal waste landfills (RCRA Subtitle D), but they contain valuable raw materials such as proppant sands. A novel process for recovering raw materials from hydraulic fracturing residual waste is presented. Specifically, a novel hydroacoustic cavitation system, combined with physical separation devices, can create a distinct stream of highly concentrated sand, and another distinct stream of clay from the residual solid waste by the dispersive energy of cavitation conjoined with ultrasonics, ozone and hydrogen peroxide. This combination cleaned the sand grains, by removing previously aggregated clays and residues from the sand surfaces. When these unit operations were followed by a hydrocyclone and spiral, the solids could be separated by particle size, yielding primarily cleaned sand in one flow stream; clays and fine particles in another; and silts in yet a third stream. Consequently, the separation of particle sizes also affected radium distribution – the sand grains had low radium activities, as lows as 0.207 Bq/g (5.6 pCi/g). In contrast, the clays had elevated radium activities, as high as 1.85 – 3.7 Bq/g (50 – 100 pCi/g) – and much of this radium was affiliated with organics and salts that could be separated from the clays. We propose that the reclaimed sand could be reused as hydraulic fracturing proppant. The

[a] Department of Civil and Environmental Engineering, the Pennsylvania State University, University Park, PA 16802, USA. Email: maa350@psu.edu.Telephone: (814)-321-4632.
[b] John and Willie Leone Family Department of Energy and Mineral Engineering, the Pennsylvania State University, University Park, PA 16802. USA
[c] Furness-Newburge, Inc., 376 Crossfield Dr., Versailles, KY 40383, USA.
[d] HydroRecovery, LP. 1975 Waddle Rd., State College, PA 16803, USA.

separation of sand from silt and clay could reduce the volume and radium masses of wastes that are disposed in landfills. This could represent a significant savings to facilities handling oil and gas waste, as much as $100,000 – $300,000 per year. Disposing the radium-enriched salts and organics downhole will mitigate radium release to the surface. Additionally, the reclaimed sand could have market value, and this could represent as much as a third of the cost savings. Tests that employed the toxicity characteristic leaching protocol (TCLP) on these separated solids streams determined that this novel treatment diminished the risk of radium mobility for the reclaimed sand, clays or disposed material, rendering them better suited for landfilling.

Keywords: sustainability; reclamation; sand; radium; hydraulic fracturing; naturally occurring radioactive material (NORM)

Introduction

Environmental sustainability is one of eight millennium development goals put forward by the United Nations; and it remains one of the biggest challenges for the current generation. Now, more than ever before, engineered solutions must be assessed through the lens of environmental sustainability. Solutions to meet the increasing energy demand of a growing population must be economically and environmentally sustainable. As our society transitions from fossil fuels to cleaner and greener energy sources, natural gas has served as an important bridge fuel toward sustainably renewable energy and a low-carbon future. This is because the burning of natural gas yields about half to two-thirds as much carbon dioxide per unit of energy generated, when compared to gasoline or coal [1].

Hydraulic fracturing has allowed for the extraction of natural gas from previously uneconomic, low-permeability formations; and this opportunity has sparked an energy revolution that is rapidly moving America towards energy independence [2]. However, this energy revolution

has not proceeded without controversy regarding issues around the relationship between hydraulic fracturing and potential environmental impacts such as: waste solids landfilling, and potential radioactivity exposure [3], elevated methane concentrations and leakage along natural gas distribution lines in urban centers [4,5], greenhouse gas emissions of methane [6–9], elevated salt impacts on streams [10–15], surface water impacts [15–18], and associated health impacts [19,20]. Groundwater methane contamination from oil and gas activities has been investigated with conflicting results: Osborn *et al.*[21] and Vengosh *et al.* [18] support this claim, while Molofsky *et al.* [22] and Siegel *et al*. [23] attribute this to natural geography. Herein, we address the first of these issues, namely, waste solids handling and management of radioactivity from hydraulic fracturing.

The handling and treatment of hydraulic fracturing waste is challenging because the liquid and solid wastes can contain elevated levels of naturally occurring radioactive material (NORM) and high concentrations of salts [24,25]. Surface discharge of partially treated liquid wastes, including flowback and produced water, has led to increased levels of metals, chloride, bromide and radioactivity in the receiving waters and sediments, as well as posing risks to aquatic and human health [10–12]. These discharges are also linked with the possibility of generating disinfectant byproducts, which are possible carcinogens, in the drinking water treatment facilities that are located further downstream [14,15,26]. Studies on the treatment of produced water for NORM removal have included sulfate precipitation (as barium or strontium sulfate) by sodium sulfate addition [27–29], or by blending with acid mine drainage [30–32]; and ion exchange using strong acid resins [33]. Sulfate precipitation remains a very effective treatment for NORM removal from produced waters, however, sulfate addition results in the generation of sludge enriched with NORM. Moreover, the dose of sulfate needed to precipitate barium (and

co-precipitated radium) is far greater with such high levels of salts – and consequently suppressed activity coefficients – than would be needed if such precipitation was occurring in freshwater that contained low salt levels [29]. Additionally, sulfate addition can result in scale formation [34] and increased activity of sulfate reducing bacteria [30] when the fluid is reused for hydraulic fracturing. While ion exchange can provide targeted radium removal, this process would require pretreatment to reduce the competition for exchange sites offered by other divalent cations.

The authors herein are not aware of published research on reclaiming the solid materials used in hydraulic fracturing, such as sand and clay, despite the considerable amounts of pristine solids consumed by this industry. A sustainable energy future includes efforts to reduce wastes that are landfilled, and strategies to recover valuable raw materials from wastes prior to disposal. Silica sand is utilized as a proppant for extending the natural fractures and maintaining higher permeability following hydraulic fracturing. The hydraulic fracturing of a single well can consume as much as 5,000 tons of sand as proppant [35]. Currently, in Pennsylvania, fracturing sands that return to the surface with flowback fluids and produced waters are disposed in landfills. In 2011, about 15,000 tons of fracturing sand were reported disposed in landfills, second after drill cuttings in disposal volume [36]. In that same year, 290 million liters (2.4 million barrels) of drilling fluids, 1 billion liters (9 million barrels) of produced water, and 940 million liters (7.9 million barrels) of flowback fluid were generated in Pennsylvania. Of that liquid waste, 70% of drilling fluids were reused and 72% of the flowback fluid and brine were reused/recycled in subsequent wells. However, we found no reported reuse/recycle of the fracturing sands [36].

The hydraulic fracturing industry has increased the demand for silica sand, and consequently, sand's price has likewise increased from about $40/ton to $87/ton in a mere 10 years (dollar values adjusted to avg. 2017 USD)[35]. Most of the fracturing sand comes from the Upper Midwest, especially Wisconsin – which in 2014 supplied almost 50% of all silica sand used for hydraulic fracturing [35]. In 2013, silica sand accounted for 85% of all proppants (by weight). This demand for sand affects other sand-using industries notably glass makers and iron foundries, who extensively use the same fine-grained silica sand from the Upper Midwest [35,37,38] (see **Figure S1**). Between 2003 and 2012, there was a 32% compound annual growth rate for silica sand used for hydraulic fracturing, in that same period, the amount of sand used for other non-fracturing uses dropped by an annual rate of 2.2%, further illustrating how the hydraulic fracturing industry is a strong market force for silica sand [35].

Economic, societal, and environmental issues related to sand mining and sand resources are growing; and these pressures have been documented in reports on the diminishing sand supply [39], land disputes [40], erosion caused by mining and transportation [35], damage to local ecosystems, increased risk of flooding [41–43], and activist protests [41,44,45]. The Appalachian Basin, of which the Marcellus Shale is a part, is the second most sand-consuming US basin[46] (following the Eagle Ford and Woodbine Formation in the East Texas Basin.) The demand for sand is expected to increase with the increased focus on developing the Marcellus Shale for natural gas and gas liquids, as well as the anticipated increased drilling of an underlying Utica Shale Formation [35].

The increased drilling activity will not only lead to greater raw material use but also greater waste volume generation. In Pennsylvania, as shown in **Figure S2,** landfills accepted almost 7,000 tons of sludge from oil and gas wastewater treatment facilities in 2017. This sludge

contains radioactive material with typical ^{226}Ra activities ranging from 0.111 Bq/g to 17.8 Bq/g (3 pCi/g to 480 pCi/g) [47,48]. Research on the treatment of such technologically enhanced naturally occurring radioactive materials (TENORM) sludge is limited [48–50]. Therefore, there is an opportunity to evaluate raw material recovery and solid waste radioactive management for the unconventional oil and gas industry.

Herein we propose to facilitate raw material recovery from unconventional oil and gas residual solid wastes by employing a novel hydroacoustic cavitation system that can also include advanced oxidation (HAC-AO). The HAC-AO system has been applied to the foundry and coal industries for raw material recovery and waste reduction; and this has pointed the way to diminished raw material use and significant savings to operating costs in both industries [52–64]. Specifically, foundries that have implemented HAC-AO have been able to save tens of millions of dollars over several decades, due to diminished sand, clay, and coal consumptions, lower air pollution, and lower scrap metal use [55,58,64]. The system (**Figure 1**) utilizes cavitation to generate localized cavities, which then collapse under ultrasonic inducement, resulting in high pressure – reported to be as high as 172 MPa (1700 atm) – and temperature – as high as 4000-5000 °K, at the nanoscale [65–67]. When the cavities are formed at the sand-clay-residue interfaces, this intense collapse causes surface debris to be pried and sheared away from such solid surfaces as sand grains, thus cleaning the sands [68]. At these localized regions, hydroxyl radicals are generated, which react aggressively with organic compounds that are present on the solid surfaces or in solution. Advanced oxidants, such as hydrogen peroxide and ozone, can be added into solution so as to increase hydroxyl radicals generation [69]. HAC-AO technology causes disaggregation of the waste particles by the dispersive energy released at bubble collapse, as well as the reactive effects of the advanced oxidants. This HAC-AO system, which consists of a cavitation-inducing

chamber and ultrasonic generator, can be coupled with a hydrocyclone and a spiral concentrator to first disaggregate sands from clays and silts, and then separate these three from one another (**Figure 1**).

In a recent publication, the underlying mechanism for HAC-AO was studied by nanoscale Surface Imaging Spectroscopy (SIS) [68]. The SIS technique provided evidence for the separation mechanism of HAC-AO, as the microscopic cleaning process for the removal of asphalt from a glass surface was observed. This study demonstrated the principles that cause the separation of sand grains from spent foundry residues.

The goal of this work was to reclaim hydraulic fracturing raw materials, while reducing landfill wastes and mitigating possible exposure to natural radium in the wastes. There were three objectives of this research. 1) To appraise a novel approach for reclaiming sand from hydraulic fracturing waste using HAC or HAC-AO, so as to reduce the volume of solid material that is disposed in landfills; 2) to evaluate the resulting radioactivity of the sands and clays that have been separated out of the waste materials following HAC or HAC-AO treatment, including leachability in a simulated landfill environment; and 3) to explore the radium affiliation within hydraulic fracturing solid materials. The hypothesis was that hydroacoustic cavitation (and/or HAC-AO) would disaggregate fine material (clays) from large grain material (sand); and following this disaggregation, physical separation devices could then create a distinct stream of recoverable, cleaned sand. As a consequence of this particle separation, we expected that higher radium activities would become affiliated with the clay-sized fractions (including dried salts and organic surfactants that could be separated from the clays); whereas lower radium activities would become affiliated with sand-sized fractions.

Materials and Methods

Sample Collection

Representative dewatered residual solid waste was collected in ~20 liters (5 gal) buckets from a hydraulic fracturing, residual waste-processing facility located in Pennsylvania. The buckets were transferred to laboratories at the Pennsylvania State University and stored at room temperature prior to testing. The water content of the residual waste was 53% by weight as determined gravimetrically and in triplicate from multiple well-mixed buckets.

Size Classification

Size classification was determined using USA standard testing sieve ASTM E-11 specification by WS Tyler Incorporated. The solids were size-classified by wet sieving through US sieve mesh #70 through #230 (212 μm to 63 μm), and immediately dried overnight in a 105 °C convection oven, after which the dry weights were recorded. All grains smaller than 63 μm, along with the wet-sieving water, were dried in the bottom pan; and this fraction thus contained some dissolved salts and organics. The samples were put into three bins based on size: +70 mesh, i.e. material retained on the #70 sieve; -70+230 mesh, i.e. material that passed through the #70 sieve but not the #230 sieve; and -230 mesh, i.e. material that passed through the #230 sieve. For simplification in discussion, material greater than sieve size #70 (+70 mesh i.e. > 212 μm) is referred to as "sand", and material less than sieve size #230 (-230 mesh i.e. <63 μm) is referred to as "clay" per ASTM D6913-04 [62]. Material between those two size fractions is referred to here as "silt".

Hydroacoustic Cavitation System

We employed a pilot-scale system that included hydroacoustic cavitation, which could be coupled with advanced oxidation (herein identified as "HAC-AO"). This system was developed

by Furness-Newburge, Inc. (Versailles, KY). Its components are scaled to pilot size and are similar to those used in industrial and sand reclaim systems as adapted under the registered trademark names of Sonoperoxone® and Pneucol®; and these modular components can be put in parallel to treat greater masses, up to 2 tons per hour. The system circuit was as shown in **Figure 1**. The system has been used by previous Penn State researchers: Liu *et al.* (2017) [61] and Barry *et al.* 2015 and 2017 [62,63]. The hydrocyclone and spiral used in these tests had been previously used by Benusa and Klima (2009) [70]. The HAC-AO system consists of a 227 L (60 gal) polyethylene conical "*feed*" tank (61 cm diameter and 107 cm height [24" diameter and 42" height]), a 5 HP centrifugal pump (3450 RPM) with Bluffon fixed-speed motor, a 11.43 cm to 15.24 cm (4.5 in by 6 in) ID and 16.51 cm (6.5 in) OD stainless steel ultrasonic chamber controlled by an ultrasonic generator operating nominally at 25 kHz with an automatic frequency control unit, and a cavitation chamber designed to cause hydrodynamic cavitation within the flow field of passing fluid. The circuit was piped with 3.81 cm (1.5 in) diameter PVC schedule 80 piping. Three way valves along the circuit enabled flow to be in the recirculation mode (without cavitation or ultrasonics) or in operation mode (with cavitation and ultrasonics).

FIG. 1.

The hydroacoustic cavitation circuit was then connected to a Krebs urethane hydrocyclone (MOD U4-in-10°) with inlet pressure of 103 kPa (15 psi). The hydrocyclone is a device used for size separations on a slurry stream. The slurry was fed tangentially via the inlet. As the slurry flowed through the hydrocyclone, centrifugal forces caused coarse particles to migrate to the wall of the hydrocyclone and out through the bottom. This material was classified as the "*underflow"*. Meanwhile, a counter vortex pushed finer particles along with the bulk of the water up through the top vortex. This material was classified as the "*overflow"*. By the principles of the hydrocyclone, the overflow will host a lower percent of solids, smaller particle

sizes, and larger flow rates, while the underflow will have a high solids percent, larger particle sizes, and lower flow rates. After separation by the hydrocyclone, the spiral concentrator was deployed to further separate the solids. A Multotex SX7 single-start two-stage seven-turn spiral concentrator was used. The spiral was operated as a closed-circuit consisting of a 5.08 cm by 3.81 cm (2 in by 1.5 in) centrifugal pump (Ash, MOD 5 ME), 15 HP motor (Westinghouse, 460 V, 1760 rpm) with variable frequency controller (ABB), and 378 L (100 gal) stainless steel sump. The spiral concentrator operated by gravity separation as the slurry flowed along the descending spiral trough. Low density particles were forced to migrate to the outer perimeter, while high-density particles migrated to the inner perimeter. After four turns, the most-dense materials were diverted into the center column, while the remaining slurry continued to flow down the trough. The splitter box, located at the end of the trough, partitioned the slurry into six streams or ports. Samples were collected at this point from each of the spiral "*ports"*. For these tests, fines were concentrated to the inner ports (1-3), while coarse-grained material was at the outer ports (4-6). The densest particles, were rejected from the first stage through the center column (port 7).

Pilot Scale Experimental Methods

The residual solids were mixed with University Park municipal tap water to prepare a 5% solids slurry, and then this slurry was sieved through US #16 mesh (1.2 mm). This tap water source was used because of its convenience at our pilot plant, and hosted negligible radium. The sieving removed grains that could otherwise clog the pump impellers; and few grains were found larger than 1.2mm. This slurry was introduced into the 50-gallon "*feed*" tank (**Figure 1**). The HAC-AO system was run as a pseudo-batch reactor: flow was recirculated from the feed tank, bypassing the cavitation box through the hydroacoustic chamber and back to the feed tank to

homogenize the material. This recirculation was done with hydroacoustic cavitation turned off. After about 2 minutes of homogenizing the material, the components of interest for each run were turned on and the system operated for 10 minutes. After this 10 minute operation, the flow was diverted to the hydroclone, where the "*underflow"* and "*overflow"* were collected in ~20 L (5 gal) buckets and a ~200 L (55 gal) drum. The overflow and underflow material were separately processed through the spiral concentrator. For each run, samples were collected from the feed tank, underflow, overflow and spiral outlet ports (see **Figure 1**). These samples were then size-classified as described above. The following experimental conditions were chosen to test the hypothesis:

1. No HAC Control: This was the Control run. The slurry was not sent through the cavitation box and the ultrasonics unit was not operating. Recirculation proceeded for 10 minutes before passing the slurry through the hydrocyclone.
2. HAC: Hydroacoustic cavitation was implemented (without ozone or hydrogen peroxide). The slurry was sent through the cavitation box and the ultrasonic unit was operating at 100% frequency power. Recirculation proceeded for 10 minutes before passing the slurry through the hydrocyclone.

Additionally, two conditions were included for further analysis to evaluate the redistribution of radium. These were:

3. HAC-AO: Hydroacoustic cavitation coupled with advanced oxidation (*AO* - hydrogen peroxide, at a dose of 0.1% (1,000 mg/L), and near-saturated ozone (at a rate of 566 L/m (20 SCFM) from an oxygen-to-ozone system). Based on prior trials, this H_2O_2 plus ozone dose in freshwater was found to generate about 0.5 – 1 mg/L of OH* radical [71].

4. HAC-LR: Hydroacoustic cavitation (no *AO*) for a longer run (*LR*) of 30 minutes operation as opposed to 10 minutes. We conducted limited tests with HAC-LR.

Representative samples from these additional runs provided further insight into the effect of HAC-AO or HAC-LR on radium management and will be further discussed.

We also collected an "As received" solid sample, which was directly sampled from multiple representative and well mixed ~20 L (5 gal) buckets. To collect a "feed" sample, we passed the 5% slurry around the recirculation loop (without HAC or AO) for 2 minutes, to achieve a uniform mix, and then collected the slurry sample from the recirculation outlet at the feed tank.

Toxicity Characteristic Leaching Procedure

The EPA Method 1311 Toxicity Characteristic Leaching Procedure (TCLP) [72] evaluated the mobility of ^{226}Ra and inorganic cations from the treated solids after HAC-AO, HAC, or the Control treatment. The TCLP is intended to mimic the chemical conditions of a landfill environment. The extraction fluid (fluid #2 – 5.7 mL glacial acetic acid diluted to a volume of 1 L using reagent water) was mixed with solid samples at a 20:1 fluid-solid mass ratio in 250 mL Nalgene® polypropylene flat bottom centrifuge tubes. After mixing for 18 hours, the suspension was centrifuged on an Eppendorf 5810R centrifuge at 3,000 RPM for 10 minutes. The supernatant was filtered through a 0.7 μm TCLP glass fiber filter (Pall Laboratory) and then transferred to a 50 mL test tube, acidified to <pH 2 with concentrated nitric acid, and stored at 4 °C until analyses using inductively coupled plasma atomic emission spectrophotometry (ICP-AES). The solid residue was then dried and the ^{226}Ra activity of this solid was determined by gamma spectroscopy (see description below).

Sequential Extractions

Radium (and major metal) association in the size-classified solids was determined by a four step sequential extraction procedure that we modified from [73] and [74]. The extractions were performed at a 20:1 fluid-to-solid mass ratio in which the extraction fluids were chosen to determine radium association with salts/evaporated pore water (Step 1: distilled–deionized water for 24 hours); with surface sites (Step 2: 1M ammonium acetate for 12 hours); with carbonate minerals (Step 3: 9% acetic acid for 12 hours); and with metal oxides (Step 4: 0.1M hydrochloric acid for 12 hours) (see **Table 1**). The initial ^{226}Ra activity, prior to Step 1 extraction, of the "As received" solids, or wet sieved, size-classified treated solids was classified as Step 0. It is noted that none of these extraction steps would dissolve barium sulfate.

The sequential extractions were carried out in 250 mL Nalgene® polypropylene flat bottom centrifuge tubes. After each extraction, the suspensions were centrifuged on an Eppendorf 5810R centrifuge at 3,000 RPM for 10 minutes, and then decanted. The pelletized solids were then rinsed with distilled-deionized water at about two-thirds the volume of the extraction fluid. All rinsates and supernatants were combined, filtered through a 0.7 μm TCLP glass fiber filter (Pall Laboratory), transferred to 50 mL test tubes, acidified to <pH 2 with concentrated nitric acid, and then refrigerated at 4 ℃ until ICP-AES analyses. The resulting pellets were oven-dried and ^{226}Ra activity in the solid was determined by gamma spectroscopy (as described below).

Table 1.

Major Metals Analyses

Elemental compositions of the acidified supernatants (Li, Na, K, Mg, Ca, Sr, Ba, Mn, Fe, and Al) were determined using ICP-AES on a Perkin-Elmer Optima 5300DV optical Emission Spectrometer per EPA standard 200.7.

Radium Analysis

Radium-226 activities of all solid samples were determined by gamma spectroscopy on a Canberra ultra-low background small anode germanium (SAGe) well detector, after the incubation period of three weeks. The reported ^{226}Ra activity was the average of the daughter products activities (^{214}Bi at 295.2 keV and 351.9 keV, ^{214}Po at 609.3 keV). The standard error was reported and the error calculation is included in the ESI. The sample geometry used was a Wheaton 24 mL poly seal cone-lined urea capped HDPE liquid scintillation vial with counting efficiencies determined using the certified UTS-2 uranium tailings provided by the Canadian Certified Reference Materials Project (CCRMP). The efficiencies of the samples were corrected for height and density, as these factors could otherwise cause a 5-40% affect in apparent ^{226}Ra activities. We monitored ^{226}Ra because it is the prominent radioactive parent in unconventional oil and gas wastes and its long half-life (1600 years) makes it persistent in the environment. Because radium's isotopes are chemically identical, the results presented for ^{226}Ra should be consistent for ^{228}Ra [75,76]. Sample masses ranged from 5 g to 35 g. To control for mass, we counted our standards within similar masses of 8g to 40 g, and develop a regression for the efficiencies at the varying masses we encountered. Counting time ranged from a few hours to a few days, because data collection was terminated either when the counting error was lower than 5% or counting time had exceeded 48 hrs. with insignificant counts. Most samples were counted once. Representative samples were tested in triplicate, and found to be within 1 – 3% of one another.

Materials

All analytical chemicals were reagent grade and supplied by VWR. Distilled de-ionized water was provided by the ThermoScientific Barnstead Nanopure water system with resistivity at 18.2 $m\Omega$. The extraction fluids for the toxicity characteristic leaching procedure and sequential

extractions were stored in glass Pyrex bottles at room temperature. Optical light microscope images were acquired on a Zeiss Axiophot microscope.

Results

Pilot Scale Trials for Raw Material Recovery

We conducted grain size analysis of the treated solids that were recovered at the "*feed*" tank, "o*verflow*", "*underflow*", and the "*spiral ports*" (**Figures 2A – 2F**). In this figure, fine particle streams will plot high and to the left, while coarse particle streams will plot low and to the right. In the No HAC Control run (**Figure 2D**), the overflow and underflow overlap – showing that the two streams had very similar particle sizes because no disaggregation had occurred. When HAC was applied (**Figure 2A**), particle disaggregation occurred – the clays were separated from the sand and the hydrocyclone successfully created two distinct streams of clay versus sand. The material collected from the overflow has plotted higher than the material collected from the underflow, indicating finer grain size in the overflow than the underflow, with both streams having distinct particle sizes from the feed material that entered the system.

FIG. 2.

In our Control run (No HAC), there was no particle disaggregation, and thus no subsequent physical separation was observed in the spiral effluents (ports 1 and 2) when processing the overflow (**Figure 2E**). Likewise, there was little physical separation observed in the spiral port 7 when processing the underflow (**Figure 2F**). In contrast, when the solids were treated with HAC, the physical separation devices successfully separated the disaggregated solids into a clay-rich stream that discharged from the overflow versus a sand-rich stream that discharged from the underflow (**Figure 2A**). Moreover, when the overflow was passed through the spiral, a clay-rich stream could be gleaned from ports 1 and 2 (**Figure 2B**), and when the underflow was passed through the spiral, a sand-rich stream could be gleaned from ports 3 and 7

(**Figure 2C**). Indeed, HAC treatment (even without AO) resulted in a particle stream from the overflow that was 82% – 88% "clays" (< 63 μm) through ports 1 and 2; and these ports constituted about 90% of all the overflow solids. Furthermore, the particle stream following HAC from the underflow was as high as 76% "sand" (> 210 μm) through port 7 and 51% though port 3 (**Figure S3**); and these ports constituted about 72% of all underflow solids. Thus, the HAC-hydrocyclone-spiral unit operations could offer a means for recovering these raw materials. With HAC-AO, the sand recovery from port 7 was 61%. Without HAC, the control offered only slight separation of sizes (**Figure S3**).

The mass balance-normalized recovery of raw materials is shown in **Table 2**. The recovery of sand through ports 3 and 7 was ~38% when treated with HAC versus only 3% for the Control – No HAC. The recovery of clays through ports 1 and 2 was ~15% when treated with HAC versus ~10% for the Control – No HAC. Without HAC treatment, the underflow contained 36% clay; compared to only 20% when treated with HAC.

Table 2.

FIG. 3.

Optical microscope images provided a visual assessment of the performance of these treatments. **Figure 3** shows the HAC-treated reclaimed sand (underflow port 7) as compared to the untreated, as-received material. As shown, the disaggregating effect of HAC treatment removed the adhered/aggregated clay particles, and yielded clean, clear sand grains. The control, without HAC, yielded grains that looked much like the "As received" material (photo not shown herein).

Toxicity Characteristic Leaching Protocol (TCLP)

The mobility of major elements and radioactivity of the selected size-classified solid waste samples was assessed using the TCLP to investigate whether HAC treatment increased the

leachability of these elements from the residual solid waste material (**Figures 4 & 5**). These results showed that radium did not leach from any of the samples, except for the "As received" clays (**Figure 4**). For all other cases, radium activities of the treated solids remained the same before and after the TCLP extraction. This indicated that there would be less risk of radium leaching from solids following treatment by HAC or HAC-AO than for solid materials that received no treatment.

FIG. 4.

We also monitored the mobility of several major elements (Li, Na, K, Mg, Ca, Sr, Ba, and Mn) that could be leached from these solids during the TCLP extraction (**Figure 5)**. Although iron and aluminum were also monitored, their concentrations were always below detection. Barium leached extensively from the "As received" material, and especially from the "As received" clays, but it did not leach significantly from any of the treated solid samples. Strontium, sodium, lithium and potassium leached the most from the "As received" and "feed" samples, and from the No HAC overflow. Calcium and magnesium leached from many of the treated samples.

When comparing **Figure 4** with **Figure 5**, we observed that radium mobility strongly followed barium mobility. Specifically, the TCLP extracted both radium and barium from the "As received" clays; but following treatment, the TCLP extracted minimal amounts of radium or barium.

Following any of these HAC or HAC-AO treatments, the barium concentration in the extractants was 0.8 mg/L to 2 mg/L (**Table S1**), compared to levels of 2 to 13.5 mg/L for the No-HAC Control. Notably, all these extractant levels following treatment were far below the TCLP regulatory limit of 500 mg/L. The concentrations of the other metals in the extractants from the

treated solids were all less than 5 mg/L, indicating that there was little potential for leaching from HAC-treated materials.

FIG. 5.

Sequential Extractions

Radium and major metal associations in the size-classified solids were determined by a four step sequential extraction procedure modified from [73,77] and [74] (**Figures 6 & 7)**. These samples were selected to represent recoverable sand (sand fraction from underflow port 7), recoverable clay (clay fraction from overflow port 1), and the intermediate silts that would be disposed (silt fraction from underflow).

FIG. 6.

For all size fractions, considerable radium was leached during step 4 – and to a lesser extent during step 3 (**Figure 6**). The cations that leached most during step 4 were Ba, Sr, Fe, and Al (**Figure 7**), indicating that radium was likely associated with their oxides. During step 3, it was the Ca, Mg, and Fe-carbonates that could be extracted – along with some radium that was associated with these carbonates. For the "As received" samples from each size-classification, the barium leached far more during steps 2, 3, and 4 than barium leached from the treated samples (**Figure 7)**.

Sequential extractions of the reclaimable sand (underflow port 7), revealed minimal radium leaching during steps 1 and 2 when HAC or HAC-AO was applied; and more radium leached during steps 3 and 4 – indicating that in the sand matrix, radium was associated with carbonate and oxide minerals (**Figure 6**). When HAC or HAC-AO was employed, the reclaimable sands had ^{226}Ra activities of ~0.74 Bq/g (20 pCi/g). Parenthetically, when HAC was operated for an extended time of 30 minutes (i.e. HAC-LR), the sand from this underflow had ^{226}Ra activities of 0.207 Bq/g (5.6 pCi/g) (**Figure S4**). Thus, the HAC-LR process could yield a

reclaimable sand that hosted low radium levels. Major metal mobility showed that calcium, magnesium, and iron were also greatly leached by step 3 (**Figure 7**). This infers that there could be some carbonate minerals in the sand-size particles leaching calcium, magnesium, iron, and aluminum. Step 4 leached barium, iron, and aluminum – inferring the presence of these oxides (**Figure 7**).

FIG. 7.

FIG. 8.

For all the clay fractions, the first extraction step (DI water) diminished radium activity, indicating that a substantial portion of the radium in these clay-sized fractions was affiliated with dissolvable salts and/or organic surfactants (**Figure 6**). Particularly, relative to the overflow port 1 "clays", organic surfactants, with their 0.85 – 0.95 mg/L density, would be expected to congregate at port 1. When the sequential extraction results (**Figure 6**) are overlapped with the major metals leached (**Figure 7**), it appears that radium was associated (at least in part) with strontium, lithium, sodium, and potassium salts (step 1); with calcium, magnesium, iron, and aluminum carbonates (step 3); and with strontium and iron oxides (step 4). Amongst these clay-rich samples, there was limited radium leaching after step 2, indicating again that radium was not associated with surface sites or low-charge clay interlayer sites.

We also monitored the mass loss that occurred during each extraction (**Figure 8**). While the dissolution of carbonate minerals during step 3 accounted for the greatest mass loss (**Figure 8**), radium did not follow this trend, as step 1 accounted for the greatest radium leaching. This is suggestive that radium association with the clays was not by interlayer adsorption but instead, radium was associated with the dried salts that had precipitated out of solution during the drying process after wet sieving – and also possibly with organic surfactants.

Finally, for the silts (underflow) that we presume will be disposed, sequential extractions showed that radium was not made more mobile following HAC-AO treatment compared to the Control samples. Although a greater portion of this HAC-AO silt fraction contained oxides (step 4) (**Figure 8**) – possibly strontium, iron, and aluminum oxides (**Figure 7**) – radium was not released during their dissolution. Metal mobility also showed the presence of calcium, magnesium, iron, and aluminum carbonates (step 3) (**Figure 7**). However, none of the treatments rendered radium more readily leachable from the silts.

Discussion

Raw material recovery: HAC treatment resulted in the disaggregation of residual solids, allowing for sand and clay separation

The market for hydraulic fracturing sand continues to grow as increased drilling activity, greater sand demand and a globally diminishing supply of suitable sand drive prices higher. It is becoming necessary to seek out alternative sources for raw materials. The quality of sand used as hydraulic fracturing proppant is specified by the API RP 19C/ISO 13503-2 standard [78]. The standard includes specifications for particle size, roundness and sphericity, among others. The HAC treatment herein resulted in the recovery of sand particles that had properties consistent with those required by the API standard. The reclaimed sand grains herein were all retained on the US #70 sieve sizes and hence could be utilized as 40/70 proppant (i.e. sand between #40 and #70 sieves). Optical microscope images revealed that these sand grains also had similar roundness and sphericity as required by the API standard. In addition, when HAC treatment was applied for 30 minutes, the radium activity on the sand grains could be as low as 0.207 Bq/g (5.6 pCi/g), which offers a reduced risk for worker exposure to radioactivity. The HAC treatment of the residual waste also resulted in the concentration of fine clays. These clays (and dried

salts/organic surfactants) were found to have high radium activities, as high as 1.85 – 3.7 Bq/g (50 – 100 pCi/g). However, more than half of the radium in these dried solids was associated with salts or organic surfactants, and was mobilized when the dried solids were suspended in DI water. These salts and surfactants could be returned back downhole with the hydraulic stimulation fluid; and they would thus not end up with landfilled solids.

We anticipate that by passing the underflow material through the HAC or HAC-AO systems a second time, we could achieve even more sand and clay recovery, as the underflow following one pass still contained 20% clays by mass when size fractioned (**Table 2**). While these clays are not presently of market value, the accumulation of radium presents an opportunity to revise the current management practices for radioactive residual waste.

Assuming a waste generation of 5,000 tons per year from such a facility as encountered by this work, HAC treatment can result in the generation of marketable source sand that could be valued around $40,000 to $80,000 per year, when sold at a fraction of the price of freshly mined sand (**Table 3**). This value can be 3 to 5 times greater if resin coated sands or ceramic proppant have been used [79]. In 2017, 6,700 tons of residual sludge waste from facilities treating oil and gas wastewater was recorded as being disposed in PA landfills (**Figure S2**). The reduction in sludge waste volume as a result of sand and clay reclamation with treatment via HAC could reduce landfill costs by about $100,000 to $300,000 per year in Pennsylvania. This is a significant cost savings for waste management operations.

Table 3.

Radium associations in the residual solids: HAC treatment diminished radium and barium mobility

The combination of the modified TCLP and sequential extractions gave insights into radium mobility and radium association in the HAC-treated residual waste solids. Firstly,

without treatment, the clay-sized particles (<63μm) showed unfavorably high potential for losing radium and barium through leaching in the landfill. After HAC-treatment, this potential was dramatically and consistently reduced for both radium and barium. Additionally, the silt-sized (between 63μm and 210μm) and sand-sized particles (>210μm), did not show potential for leaching radium or barium following HAC or HAC-AO treatments. Radium associations in the residual waste before treatment indicated that radium was most mobile from the particle sizes less than 63μm and should be further evaluated prior to disposal.

An interesting finding was that radium was removed during step 1 of the sequential extractions, and thus perceived as being associated with dried salts or organic surfactants in this residual waste. This residual waste was collected from a facility that does not treat the wastewater with sulfate addition for radium control. There are a number of such facilities with similar operations that handle oil and gas waste. The residual solids coming from such facilities are likely to have similar radium associations.

It is possible that radium was complexed with organic compounds in this material. Such compounds could be surfactants, acetate, and EDTA. These (and especially surfactants) are used during hydraulic fracturing; and they have been detected in flowback and produced water [25,81,82]. We observed the presence of organics (enough to form a surface sheen) in the waste and slurry used in the HAC treatment; and this would be indicative that surfactants are present. Moreover, the combination of cavitation and bubbled ozone resulted in dissolved air that accumulated in the ultrasonic chamber, and apparently created a similar phenomenon as for a small-scale dissolved-air flotation unit. This resulted in the agglomeration of an organic-rich clay in samples collected from HAC and especially HAC-AO treatments. As these samples dried, we infer that the radium that had been complexed by these organic compounds became associated with the clays. The

operation of the HAC system would have caused these organic-rich clays to be concentrated in the overflow and subsequently in spiral ports 1 and 2. This could be an explanation of the very high radium activity found in the clays from HAC-AO overflow port 1. The sequential extraction of these clays showed radium mobility following the first step (DI water). Our prior research with foundry green sand indicated that HAC-AO released organic residues from solid surfaces [56,68]. Thus, such radium-rich organic compounds, as well as salts, could be separated from the clays, and returned back downhole with hydraulic stimulation fluids. We note that the chemical oxygen demand (COD) of the extractant following this step was determined to be 1,300 mg/L; indicating that indeed anionic organic surfactants, which are known to complex cationic radium [83], could in part explain the mobility of radium. In overview, the combination of radium association with salts and organics presents an opportunity for the development of new radium management practices of such residual solids.

Implications for disposal

The Pennsylvania Department of Environmental Protection (PA DEP) commissioned a study to investigate exposure and contamination risks from TENORM at facilities impacted by oil and gas operations [47]. The average radium activity reported by this PA DEP study for proppant sand prior to hydraulic fracturing was 8.99 Bq/kg $\pm$ 2.18 (243 pCi/kg $\pm$ 59), and after was 128 Bq/kg $\pm$ 110 (3460 pCi/kg $\pm$ 2990); while the filter cake (i.e., sludge) of nine zero liquid discharge facilities had activities that ranged from 0.111 Bq/g to 17.8 Bq/g (3 pCi/g to 480 pCi/g) [47]. The reclaimed sand from our work had radium activity as low as 0.207 Bq/g (5.6 pCi/g), with little risk for leaching of this radium; while the reclaimed clays (including salts and organics) could be as high as 3.7 Bq/g (100 pCi/g). The activity of the eventually disposed material ranged from 0.74 Bq/g to 1.48 Bq/g (20 pCi/g to 40 pCi/g). The disposed material will

thus contain lower net radium mass and lower volume, thereby reducing TENORM waste disposal and landfill costs. Alternative treatment for solid waste management with elevated radioactivity can be proposed following the findings from the TCLP and sequential extractions. Radium in the residual solids was associated with salts, carbonates, oxides, and possibly surfactants at this study site.

Limitations of this study

In this work, municipal tap water was used to make the slurries prior to experimental runs on the HAC system. This protocol was an inherent artefact of conducting these pilot-scale tests at Penn State, miles from the residual waste-processing facility. We acknowledge that such intentional dilution would be impractical for a full-scale operation. Instead high-TDS produced and flowback water would be present in any on-site slurries.

The fate of several heavy metals was not evaluated; however, non-heavy metal concentrations of Fe, Al, and Mn in extraction fluids following the TCLP and sequential extractions suggest that heavy metal concentration will be relatively low. Reported heavy metal concentration in Marcellus Shale produced fluids are <1mg/L, compared to barium, calcium, and magnesium at 50 – 30,000 mg/L [25,84]. The concentrations of these metals (Ba, Ca, and Mg) in the extractants did not exceed 5 mg/L, therefore it is not expected that the heavy metals will have significant concentrations. Additionally, we did not attempt to quantify the effect of treatment or the leaching potential of these solids for other radionuclides such as Uranium (U). Eitrheim *et al.*[85] found that U was mobile from Appalachian drilling wastes when the TCLP was applied. U could also have been released by these solids given the sonication, cavitation, and oxidation processes involved herein.

Conclusions and recommendations

A novel process for recovering raw material from oil and gas residual waste was presented using hydroacoustic cavitation and advanced oxidants, combined with physical separation devices to create distinct streams of highly concentrated sand and clay. The separation of particles sizes affected radium distribution – the sand grains had low radium activities, as low as 0.185 – 0.74 Bq/g (5 – 20 pCi/g); whereas the clays (along with their associated salts and organics) had elevated radium activities, as high as 1.85 – 3.7 Bq/g (50 – 100 pCi/g). We propose that the sand grains can be reused as recycled hydraulic fracturing proppant. The separation of sand from clay and silt could reduce the volume of radium-containing wastes that are disposed in landfills, and also reduce the radium mass to landfills. This could represent a significant savings to facilities handling unconventional oil and gas waste. Additionally, the reclaimed sand could have market value in hydraulic fracturing drilling, or in other silica sand-using industries. Although the clays (and associated salts and organics) are currently of little market value, their elevated radium activity presents an opportunity to revise current waste handling practices for radioactive management. Disposing these radium-enriched salts and dislodged organic compounds downhole with hydraulic fracturing fluid will lower radium exposure and therefore risk to human health and the environment. Extractions performed on the residual waste indicated that in facilities that do not perform sulfate precipitation, radium is likely to be associated with dried salts and organic compounds.

The continued development of the Marcellus Shale and the underlying Utica Shale will result in greater use of raw materials and greater volume of solid and liquid waste. The Utica Shale is estimated to produce 2.5 times more produced water per unit gas than the Marcellus Shale [86]. These produced waters will contain NORM that could otherwise end up in

impoundment sludge or water treatment sludge. If not mitigated, the continued recycling of produced water for hydraulic fracturing could cause an increase in TDS and radium activities [48], potentially increasing the radioactivity and volume of sludge generated during treatment. This work provides evidence that when these solids (sands, suspended solids, and sludge) are collected in a waste handling facility, hydroacoustic cavitation with advanced oxidation followed by physical separation devices can be applied to (a) reclaim the sands with lowered radioactivity; (b) separate the clays, salts and organics with high activity, and (c) reduce the potential of radium leaching from the solids that require disposal.

Acknowledgments

This research was funded by a National Science Foundation PFI: AIR-TT #1640634. Further support originated from a Penn State College of Engineering Graduate Excellence Fellowship. We acknowledge Hydro Recovery LP for providing the samples used in this study.

Author disclosure statement

No competing financial interests exist.

References

1 R. A. Kerr, Energy. Natural gas from shale bursts onto the scene., *Science*, 2010, **328**, 1624–6.

2 U.S. Energy Information Administration, *Annual Energy Outlook*, Washington, DC, 2018.

3 D. M. Kargbo, R. G. Wilhelm and D. J. Campbell, Natural Gas Plays in the Marcellus Shale: Challenges and Potential Opportunities, *Environ. Sci. Technol.*, 2010, **44**, 5679–5684.

4 M. E. Gallagher, A. Down, R. C. Ackley, K. Zhao, N. Phillips and R. B. Jackson, Natural Gas Pipeline Replacement Programs Reduce Methane Leaks and Improve Consumer Safety, *Environ. Sci. Technol. Lett.*, 2015, **2**, 286–291.

5 K. McKain, A. Down, S. M. Raciti, J. Budney, L. R. Hutyra, C. Floerchinger, S. C. Herndon, T. Nehrkorn, M. S. Zahniser, R. B. Jackson, N. Phillips and S. C. Wofsy, Methane emissions from natural gas infrastructure and use in the urban region of Boston, Massachusetts., *Proc. Natl. Acad. Sci. U. S. A.*, 2015, **112**, 1941–6.

6 G. Heath, J. Meldrum, N. Fisher, D. Arent and M. Bazilian, Life cycle greenhouse gas emissions from Barnett Shale gas used to generate electricity, *J. Unconv. Oil Gas Resour.*, 2014, **8**, 46–55.

7 R. W. Howarth, R. Santoro and A. Ingraffea, Methane and the greenhouse-gas footprint of natural gas from shale formations, *Clim. Change*, 2011, **106**, 679–690.

8 R. W. Howarth, A. Ingraffea and T. Engelder, Should fracking stop?, *Nature*, 2011, **477**, 271–275.

9 M. Jiang, W. Michael Griffin, C. Hendrickson, P. Jaramillo, J. VanBriesen and A. Venkatesh, Life cycle greenhouse gas emissions of Marcellus shale gas, *Environ. Res.*

Lett., 2011, **6**, 34014.

10 N. R. Warner, C. A. Christie, R. B. Jackson and A. Vengosh, Impacts of shale gas wastewater disposal on water quality in Western Pennsylvania, *Environ. Sci. Technol.*, 2013, **47**, 11849–11857.

11 K. J. Ferrar, D. R. Michanowicz, C. L. Christen, N. Mulcahy, S. L. Malone and R. K. Sharma, Assessment of effluent contaminants from three facilities discharging marcellus shale wastewater to surface waters in Pennsylvania, *Environ. Sci. Technol.*, 2013, **47**, 3472–3481.

12 J. M. Wilson and J. M. Van Briesen, Source Water Changes and Energy Extraction Activities in the Monongahela River, 2009–2012, *Environ. Sci. Technol.*, 2013, **47**, 12575–12582.

13 J. M. Wilson, Y. Wang and J. M. VanBriesen, Sources of High Total Dissolved Solids to Drinking Water Supply in Southwestern Pennsylvania, *J. Environ. Eng.*, 2014, **140**, B4014003-1-B4014003-10.

14 J. M. Wilson and J. M. VanBriesen, Oil and Gas Produced Water Management and Surface Drinking Water Sources in Pennsylvania, *Environ. Pract.*, 2012, **14**, 288–300.

15 K. M. Parker, T. Zeng, J. Harkness, A. Vengosh and W. A. Mitch, Enhanced Formation of Disinfection Byproducts in Shale Gas Wastewater-Impacted Drinking Water Supplies, *Environ. Sci. Technol.*, 2014, **48**, 11161–11169.

16 W. D. Burgos, L. Castillo-Meza, T. L. Tasker, T. J. Geeza, P. J. Drohan, X. Liu, J. D. Landis, J. Blotevogel, M. McLaughlin, T. Borch and N. R. Warner, Watershed-Scale Impacts from Surface Water Disposal of Oil and Gas Wastewater in Western Pennsylvania, *Environ. Sci. Technol.*, 2017, **51**, 8851–8860.

17 J. S. Harkness, G. S. Dwyer, N. R. Warner, K. M. Parker, W. A. Mitch and A. Vengosh, Iodide, bromide, and ammonium in hydraulic fracturing and oil and gas wastewaters: Environmental implications, *Environ. Sci. Technol.*, 2015, **49**, 1955–1963.

18 A. Vengosh, R. B. Jackson, N. R. Warner, T. H. Darrah and A. Kondash, A Critical Review of the Risks to Water Resources from Unconventional Shale Gas Development and Hydraulic Fracturing in the United States, *Environ. Sci. Technol.*, 2014, **48**, 8334–8348.

19 J. Kravchenko, T. H. Darrah, R. K. Miller, H. K. Lyerly and A. Vengosh, A review of the health impacts of barium from natural and anthropogenic exposure, *Environ. Geochem. Health*, 2014, **36**, 797–814.

20 L. Konkel, Salting the Earth: The Environmental Impact of Oil and Gas Wastewater Spills, *Environ. Health Perspect.*, 2016, **124**, A230–A235.

21 S. G. Osborn, A. Vengosh, N. R. Warner and R. B. Jackson, Methane contamination of drinking water accompanying gas-well drilling and hydraulic fracturing., *Proc. Natl. Acad. Sci. U. S. A.*, 2011, **108**, 8172–6.

22 L. J. Molofsky, J. A. Connor, A. S. Wylie, T. Wagner and S. K. Farhat, Evaluation of Methane Sources in Groundwater in Northeastern Pennsylvania, *Groundwater*, 2013, **51**, 333–349.

23 D. I. Siegel, N. A. Azzolina, B. J. Smith, A. E. Perry and R. L. Bothun, Methane Concentrations in Water Wells Unrelated to Proximity to Existing Oil and Gas Wells in Northeastern Pennsylvania, *Environ. Sci. Technol.*, 2015, **49**, 4106–4112.

24 E. L. Rowan, M. A. Engle, T. F. Kraemer, K. T. Schroeder, R. W. Hammack and M. W. Doughten, Geochemical and isotopic evolution of water produced from Middle Devonian

Marcellus shale gas wells, Appalachian basin, Pennsylvania, *Am. Assoc. Pet. Geol. Bull.*, 2015, **99**, 181–206.

25 T. Hayes, *Sampling and Analysis of Water Streams Associated with the Development of Marcellus Shale Gas*, Marcellus Shale Coalition Final Report, Des Plaines, 2009.

26 K. D. Good and J. M. VanBriesen, Current and Potential Future Bromide Loads from Coal-Fired Power Plants in the Allegheny River Basin and Their Effects on Downstream Concentrations, *Environ. Sci. Technol.*, 2016, **50**, 9078–9088.

27 C. He, M. Li, W. Liu, E. Barbot and R. D. Vidic, Kinetics and Equilibrium of Barium and Strontium Sulfate Formation in Marcellus Shale Flowback Water, *J. Environ. Eng.*, 2014, **140**, B4014001-1-B4014001-9.

28 T. Zhang, K. Gregory, R. W. Hammack and R. D. Vidic, Co-precipitation of radium with barium and strontium sulfate and its impact on the fate of radium during treatment of produced water from unconventional gas extraction, *Environ. Sci. Technol.*, 2014, **48**, 4596–4603.

29 M. I. Zermeno-Motante, C. Nieto-Delgado, F. S. Cannon, C. C. Cash and C. C. Wunz, Chemical modeling for precipitation from hypersaline hydrofracturing brines, *Water Res.*, 2016, **103**, 233–244.

30 C. He, T. Zhang and R. D. Vidic, Use of Abandoned Mine Drainage for the Development of Unconventional Gas Resources, *Disruptive Sci. Technol.*, 2013, **1**, 169–176.

31 C. He, T. Zhang and R. D. Vidic, Co-treatment of abandoned mine drainage and Marcellus Shale flowback water for use in hydraulic fracturing, *Water Res.*, 2016, **104**, 425–431.

32 C. He, T. Zhang, X. Zheng, Y. Li and R. D. Vidic, Management of Marcellus Shale

Produced Water in Pennsylvania: A Review of Current Strategies and Perspectives, *Energy Technol.*, 2014, **2**, 968–976.

33 Y. Bi, H. Zhang, B. R. Ellis and K. F. Hayes, Removal of Radium from Synthetic Shale Gas Brines by Ion Exchange Resin, *Environ. Eng. Sci.*, 2016, **33**, 791–798.

34 A. N. Paukert Vankeuren, J. A. Hakala, K. Jarvis and J. E. Moore, Mineral Reactions in Shale Gas Reservoirs: Barite Scale Formation from Reusing Produced Water As Hydraulic Fracturing Fluid, *Environ. Sci. Technol.*, 2017, **51**, 9391–9402.

35 M. E. Benson and A. B. Wilson, *Frac Sand in the United States—A Geological and Industry Overview*, U.S. Geological Survey Open-File Report 2015–1107, DOI: 10.3133/ofr20151107, 2015.

36 K. O. Maloney and D. A. Yoxtheimer, Production and Disposal of Waste Materials from Gas and Oil Extraction from the Marcellus Shale Play in Pennsylvania, *Environ. Pract.*, 2012, **14**, 278–287.

37 U.S. Geological Survey (USGS), Industrial sand and gravel, in Metals and minerals: U.S. Geological Survey Minerals Yearbooks 1991–2017, various pagination, http://minerals.usgs.gov/ minerals/pubs/usbmmyb.html and http://minerals.usgs.gov/ minerals/pubs/commodity/silica/, (accessed 17 February 2018).

38 Baker-Hughes Inc, Baker-Hughes Rig count: North America Rig Count, http://phx.corporate-ir.net/phoenix.zhtml?c=79687&p=irol-reportsother, (accessed 20 February 2018).

39 V. Beiser, The World's Disappearing Sand, https://www.nytimes.com/2016/06/23/opinion/the-worlds-disappearing-sand.html, (accessed 17 February 2018).

40 T. W. Pearson, Frac Sand Mining in Wisconsin: Understanding Emerging Conflicts and Community Organizing, *Cult. Agric. Food Environ.*, 2013, **35**, 30–40.

41 V. Beiser, The Deadly Global War for Sand, https://pulitzercenter.org/reporting/india-deadly-global-war-sand, (accessed 17 February 2018).

42 V. Beiser, How Sand Mining Helped Flood Houston, https://pulitzercenter.org/reporting/how-sand-mining-helped-flood-houston, (accessed 17 February 2018).

43 V. Beiser, Sand mining: the global environmental crisis you've never heard of, https://www.theguardian.com/cities/2017/feb/27/sand-mining-global-environmental-crisis-never-heard, (accessed 17 February 2018).

44 V. Beiser, India: The Deadly Global War for Sand, https://pulitzercenter.org/reporting/india-deadly-global-war-sand, (accessed 17 February 2018).

45 V. Beiser, He who controls the sand: the mining 'mafias' killing each other to build cities, https://www.theguardian.com/cities/2017/feb/28/sand-mafias-killing-each-other-build-cities, (accessed 17 February 2018).

46 D. Bleiwas, Estimates of hydraulic fracturing (Frac) sand production, consumption, and reserves in the United States., https://www.thefreelibrary.com/Estimates+of+hydraulic+fracturing+(Frac)+sand+production%2C...-a0418603320, (accessed 20 February 2018).

47 Pennsylvania Department of Environmental Protection (PA DEP), Technologically Enhanced Naturally Occurring Radioactive Materials (TENORM) Study Report, http://www.depgreenport.state.pa.us/elibrary/getdocument?docid=5815&docname=01

pennsylvania department of environmental protection tenorm study report rev 1.pdf, (accessed 8 February 2018).

48 T. Zhang, R. W. Hammack and R. D. Vidic, Fate of Radium in Marcellus Shale Flowback Water Impoundments and Assessment of Associated Health Risks, *Environ. Sci. Technol.*, 2015, **49**, 9347–9354.

49 M. F. Attallah, M. M. Hamed, E. M. El Afifi and H. F. Aly, Removal of226Ra and228Ra from TENORM sludge waste using surfactants solutions, *J. Environ. Radioact.*, 2015, **139**, 78–84.

50 W. M. Kappel, J. H. Williams and Z. Szabo, *Water Resources and Shale Gas/Oil Production in the Appalachian Basin—Critical Issues and Evolving Developments*, U.S. Geological Survey Open-File Report 2013–1137, 2013.

51 Pennsylvania Department of Environmental Protection (PA DEP), PA DEP Oil and Gas Reporting Website: Statewide Data Downloads by Reporting Period, https://www.paoilandgasreporting.state.pa.us/publicreports/Modules/Welcome/ProdWasteReports.aspx, (accessed 20 February 2018).

52 J. T. Fox, F. S. Cannon, R. C. Voigt, P. B. Smith, S. E. Lewallen and J. E. Goudzwaard, Simultaneous Sand , Clay and Coal Reclamation Using Induced Particle Collision , Discretionary Settling and Advanced Oxidation, *Trans. Am. Foundry Soc.*, 2007, **115**, 1–16.

53 J. T. Fox, F. S. Cannon, R. C. Voigt, J. C. Furness, F. Headington, D. Coan and S. Lewallen, Waste Green Sand to Core Sand Reclamation, Demonstration via Casting Study with Simultaneous Clay Recovery via a Novel Ultrasonic-Cavitation System, *Trans. Am. Foundry 116*, 2008, **116**, 523–538.

54 J. T. Fox, F. S. Cannon, R. C. Voigt, J. E. Goudzwaard, M. Wosoba and P. B. Smith, Decreased Bond Consumption by Processing Baghouse Dust through Ultrasonic-Cavitation-Settling Coupled to Advanced Oxidation, *Trans. Am. Foundry Soc.*, 2008, **116**, 539–546.

55 J. E. Goudzwaard, C. M. Kurtti, J. H. Andrews, F. S. Cannon, R. C. Voigt, J. E. Firebaugh, J. C. Furness and D. L. Sipple, Foundry Emissions Effects with an Advanced Oxidation Blackwater System, *Trans. Am. Foundry Soc.*, 2003, **111**, 1191–1211.

56 Y. Wang, F. S. Cannon, S. Komarneni, R. C. Voigt and J. C. Furness, Mechanisms of advanced oxidation processing on bentonite consumption reduction in foundry, *Environ. Sci. Technol.*, 2005, **39**, 7712–7718.

57 C. R. Glowacki, G. R. Crandell, F. S. Cannon, J. K. Clobes, R. C. Voigt, J. C. Furness, B. A. McComb and S. M. Knight, Emissions Studies at a Test Foundry using an Advanced Oxidation-Clear Water System, *Trans. Am. Foundry Soc.*, 2003, **111**, 579–598.

58 D. A. Neill, F. S. Cannon, R. C. Voigt, J. C. Furness and R. H. Bigge, Effects of Advanced Oxidants on Green Sand System in a Black Water System, *Trans. Am. Foundry Soc.*, 2001, **109**, 1–19.

59 J. D. Land, R. C. Voigt, F. S. Cannon, J. C. Furness, J. Goudzwaard and H. Luebben, Performance and Control of a Green Sand System During the Installation and Operation of an Advanced Oxidation System., *Trans. Am. Foundry Soc.*, 2002, **110**, 705–713.

60 J. Andrews, R. Bigge, F. S. Cannon, G. R. Crandell, Furness J.C., M. Redmann and R. C. Voigt, Advanced oxidants offer opportunities to improve mold properties, emissions, *Mod. Cast.*, 2000, **90**, 40.

61 S. Liu, T. Geeza, F. S. Cannon, M. S. Klima, J. C. Furness and J. Pagnotti, Hydroacoustic

Cavitation for Recovering Anthracite Fines from Waste Silt Slurry, *J. Min. World Express*, 2017, **6**, 10.

62 B. Barry, M. S. Klima and F. S. Cannon, Effect of hydroacoustic cavitation treatment on the spiral processing of bituminous coal, *Int. J. Coal Prep. Util.*, 2015, **35**, 76–87.

63 B. Barry, M. S. Klima and F. S. Cannon, Effects of Desliming and Hydroacoustic Cavitation Treatment on the Flotation of Ultrafine Bituminous Coal, *Int. J. Coal Prep. Util.*, 2017, **37**, 213–224.

64 R. M. Torielli, F. S. Cannon, R. C. Voigt, T. J. Considine, J. C. Furness, J. T. Fox, J. E. Goudzwaard and H. Huang, The Environmental Performance and Cost of Innovative Technologies for Ductile Iron Foundry Production, *Int. J. Met.*, 2014, **8**, 37–48.

65 E. B. Flint and K. S. Suslick, The temperature of cavitation., *Science*, 1991, **253**, 1397–1399.

66 Y. T. Didenko, W. B. McNamara and K. S. Suslick, Temperature of multibubble sonoluminescence in water, *J. Phys. Chem. A*, 1999, **103**, 10783–10788.

67 T. J. Mason and D. Peters, in *Practical Sonochemistry*, Horwood Publishing Limited, Chichester, 2nd edn., 2002, vol. 1, ch. 1, pp. 12.

68 X. Y. S. Zhang, M. A. Ajemigbitse, F. S. Cannon, A. E. Hooper, D. L. Allara, P. D. Paulsen and J. C. Furness, Hydrogen Peroxide-Generated Gases at Asphalt-Glass Interface: Effect on Surface Cleaning and Analysis by Nanoscale Surface Imaging Spectroscopy, *Environ. Eng. Sci.*, 2018, **35**, 300–310.

69 T. J. Mason and J. P. Lorimer, in *Applied Sonochemistry*, Wiley-VCH, Weinheim, 1st edn., 2002, vol. 1, ch. 2, pp. 36-38.

70 M. D. Benusa and M. S. Klima, An Evaluation of a Two-Stage Spiral Processing Fine

Anthracite Refuse, *Int. J. Coal Prep. Util.*, 2009, **29**, 49–67.

71 N. Milan-Segovia, Y. Wang, F. S. Cannon, R. C. Voigt and J. C. Furness, Comparison of Hydroxyl Radical Generation for Various Advanced Oxidation Combinations as Applied to Foundries, *Ozone Sci. Eng.*, 2007, **29**, 461–471.

72 Environmental Protection Agency (EPA), EPA Test Method 1311 - Toxicity Characteristic Leaching Procedure (TCLP), https://www.epa.gov/sites/production/files/2015-12/documents/1311.pdf, (accessed 5 September 2017).

73 T. L. Tasker, P. K. Piotrowski, F. L. Dorman and W. D. Burgos, Metal Associations in Marcellus Shale and Fate of Synthetic Hydraulic Fracturing Fluids Reacted at High Pressure and Temperature, *Environ. Eng. Sci.*, 2016, **33**, 753–765.

74 B. W. Stewart, E. C. Chapman, R. C. Capo, J. D. Johnson, J. R. Graney, C. S. Kirby and K. T. Schroeder, Origin of brines, salts and carbonate from shales of the Marcellus Formation: Evidence from geochemical and Sr isotope study of sequentially extracted fluids, *Appl. Geochemistry*, 2015, **60**, 78–88.

75 International Atomic Energy Agency (IAEA), *The Environmental Behaviour of Radium: Revised Edition. Technical Report Series no. 476*, Vienna, 2014.

76 A. W. Nelson, E. S. Eitrheim, A. W. Knight, D. May, M. A. Mehrhoff, R. Shannon, R. Litman, W. C. Burnett, T. Z. Forbes and M. K. Schultz, Understanding the Radioactive Ingrowth and Decay of Naturally Occurring Radioactive Materials in the Environment : An Analysis of Produced Fluids from the Marcellus Shale, *Environ. Health Perspect.*, 2015, **123**, 689–696.

77 A. W. Nelson, A. J. Johns, E. S. Eitrheim, A. W. Knight, M. Basile, E. A. Bettis III, M. K.

Schultz and T. Z. Forbes, Partitioning of naturally-occurring radionuclides (NORM) in Marcellus Shale produced fluids influenced by chemical matrix, *Environ. Sci. Process. Impacts*, 2016, **18**, 456–463.

78 American Petroleum Institute, *API RP 19C/ISO 13503-2: "Recommended Practice for Measurement of Properties of Proppants Used in Hydraulic Fracturing and Gravel-packing Operations"*, American Petroleum Institute (API), Washington DC, 1st edn., 2008.

79 Carbo Ceramics, personal communication.

80 D. Shin, M.S. Thesis, Columbia University, 2014.

81 J. L. Luek and M. Gonsior, Organic compounds in hydraulic fracturing fluids and wastewaters: A review, *Water Res.*, 2017, **123**, 536–548.

82 D. M. Akob, I. M. Cozzarelli, D. S. Dunlap, E. L. Rowan and M. M. Lorah, Organic and inorganic composition and microbiology of produced waters from Pennsylvania shale gas wells, *Appl. Geochemistry*, 2015, **60**, 116–125.

83 A. V. Matyskin, N. L. Hansson, P. L. Brown and C. Ekberg, Barium and Radium Complexation with Ethylenediaminetetraacetic Acid in Aqueous Alkaline Sodium Chloride Media, *J. Solution Chem.*, 2017, **46**, 1951–1969.

84 N. Abualfaraj, P. L. Gurian and M. S. Olson, Characterization of Marcellus Shale Flowback Water, *Environ. Eng. Sci.*, 2014, **31**, 514–524.

85 E. S. Eitrheim, D. May, T. Z. Forbes and A. W. Nelson, Disequilibrium of Naturally Occurring Radioactive Materials (NORM) in Drill Cuttings from a Horizontal Drilling Operation, *Environ. Sci. Technol. Lett.*, 2016, **3**, 425–429.

86 R. D. Vidic and D. Yoxtheimer, presented in part at the 2017 Shale Network Workshop,

842 State College, May, 2017.

843

PennState
Department of Civil and Environmental Engineering
College of Engineering
The Pennsylvania State University
212 Sackett Building
University Park, PA 16802-1408
814-863-3084
Fax: 814-863-7304
www.cee.psu.edu

FIG. 1. The Furness Newburge hydroacoustic cavitation circuit showing process flow and components (not to scale). Slurry from the *feed tank* was circulated through the cavitation box and hydroacoustic cavitation chamber for treatment. Following treatment, the slurry was pumped to the *hydroclone*: slurry came in through the inlet and two outflow streams were created: the underflow – with larger grains and higher solids concentration; and the overflow – with smaller grains and lower solids concentration. The hydrocyclone separated particles by size – fines were diverted to the overflow while coarser particles were diverted to the underflow. Next was the *spiral concentrator*: the underflow or overflow slurry was pumped upward from the sump to the top of the stack. Separation by gravity occurred as the slurry flowed downward through the spiral trough. The repulper at the end of the first stage (after 4 turns) rejected very coarse material into the central column (port 7). The remaining slurry passed over the final 4 turns and discharged through the spiral ports. The spiral separated particles primarily by density – low-density particles were diverted to ports 1 & 2, while high-density particles were diverted to ports 3-7. Red boxes denote sampling points. After [62] and [70].

FIG. 2. Grain size analysis of HAC treatment (without AO – panels **A**, **B**, & **C**) and Control (No HAC – panels **D**, **E** & **F**) of solids collected at sampling points downstream of the treatment system. Fine particles will plot high and to the left, while coarse particles will plot low and to the right. Grain size analysis performed using US mesh sieves per ASTM D6913-04 from < 63 μm (#230 mesh i.e. clay) to >210 μm (#70 mesh i.e. sand). HAC causes disaggregation of homogenized solids when processing dewatered residual solids in 5% slurry with municipal tap water (for HAC treatment (panel **A)** compared to the No HAC Control (panel **D**)). Fine particles go to the overflow and large particles go to the underflow. Disaggregated solids can be further separated by the cyclone and spiral – with HAC, the process achieved higher concentration of clay (panel **B** vs **E**) and sand (panel **C** vs **F**). HAC treatment results in a distinct particle size distribution.

FIG. 3. Optical light microscopy (Zeiss Axiophot microscope) provided visual assessment of the "As received" sand grains aggregated with clays and fines on their surfaces (left panel), compared to the HAC treatment (right panel), which was effective at disaggregating the clay fines off the sand. Further physical separation devices resulted in reclaimed sand that was free of clays and silts.

PennState
Department of Civil and Environmental Engineering
College of Engineering
The Pennsylvania State University
212 Sackett Building
University Park, PA 16802-1408
814-863-3084
Fax: 814-863-7304
www.cee.psu.edu

FIG. 4. Radium-226 activities on the size-classified solids from various sample ports: initial and post TCLP extraction. Radium-226 activities (Bq) have been normalized to initial mass (g) of the solid prior to extraction. Error bars denote combined standard error in radium measurements and mass measurements. Samples were taken from the feed, hydrocyclone, underflow (under), and overflow (over). Red boxes highlight HAC-AO treatment. Size classification using US mesh sieves per ASTM D6913-04: $< 63\ \mu m$ is clay (#230 mesh), $>210\ \mu m$ is sand (#70 mesh), and in-between is silt. Radium leached significantly from the "As Received" clay sized solids. These results indicated that treatment diminished the risk of radium leaching out in the landfill.

FIG. 5. Major metal mobility of the size-classified samples following TCLP extraction, in mg metal extracted per initial g of solids. Samples were taken from the feed, hydrocyclone, underflow (under), and overflow (over). Radium mobility strongly followed barium mobility. Leaching did not result in concentrations above regulatory limits for TCLP and landfill disposal.

FIG. 6. Radium-226 activities of the sequentially extracted, size-classified, treated solids. Radium-226 activities (Bq) have been normalized to initial mass (g) of the solid prior to extraction. Error bars denote combined standard error in radium measurements and mass measurements. Step 0 (■): Initial solid; Step 1 (■): DI water rinse for soluble salts; Step 2 (■): 1 M ammonium acetate for surface sites; Step 3 (■): 9% acetic acid for carbonates; Step 4 (■): 0.1 M hydrochloric acid for oxides. shading for sand, for silt, and for clay. The "As received" samples are demarcated with a lighter shade.

FIG. 7. Major metal mobility of the size-classified, sequentially extracted samples in mg metal extracted per g of solids prior to each extraction step. Step 1 (■): DI water rinse for soluble salts; Step 2 (■): 1M ammonium acetate for surface sites; Step 3 (■): 9% acetic acid for carbonates; Step 4 (■): 0.1 M hydrochloric acid for oxides. shading for sand, for silt, and for clay. The "As received" samples are demarcated with a lighter shade.

FIG. 8. Mass lost from the size-classified solids following sequential extractions. Step 1 (■): DI water rinse for soluble salts; Step 2 (■): 1M ammonium acetate for surface sites; Step 3 (■): 9% acetic acid for carbonates; Step 4 (■): 0.1 M hydrochloric acid for oxides; and Recalcitrant mass (■) following steps 1-4. shading for sand, for silt, and for clay. The "As received" samples are demarcated with a lighter shade.

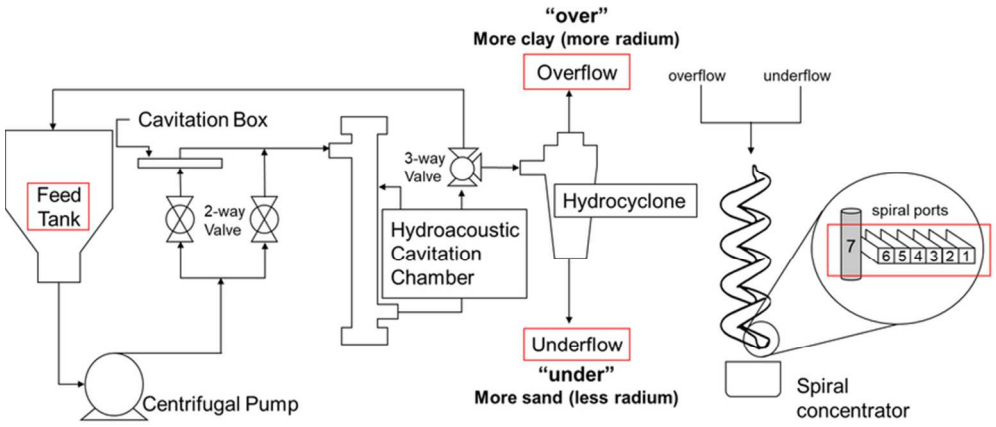

Figure 1

74x32mm (300 x 300 DPI)

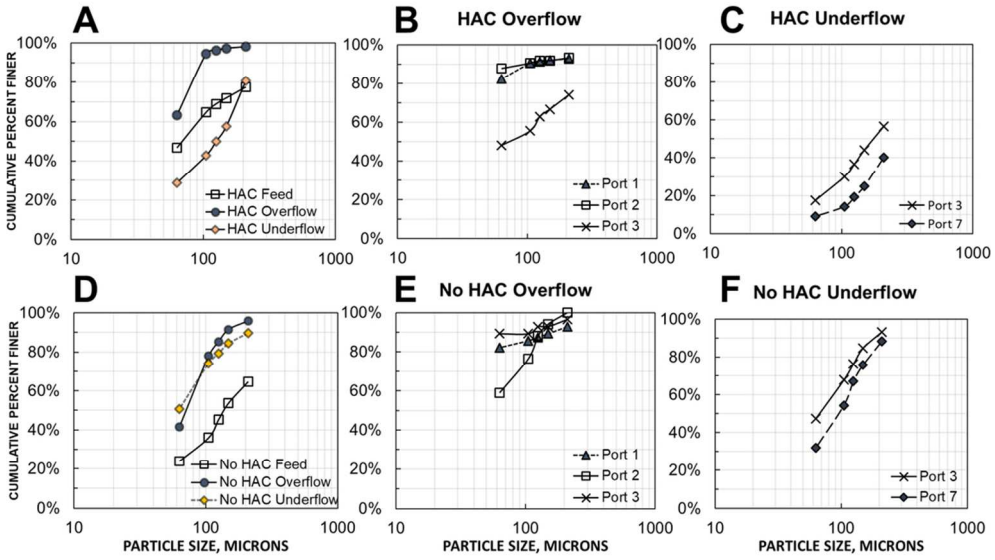

Figure 2

98x56mm (300 x 300 DPI)

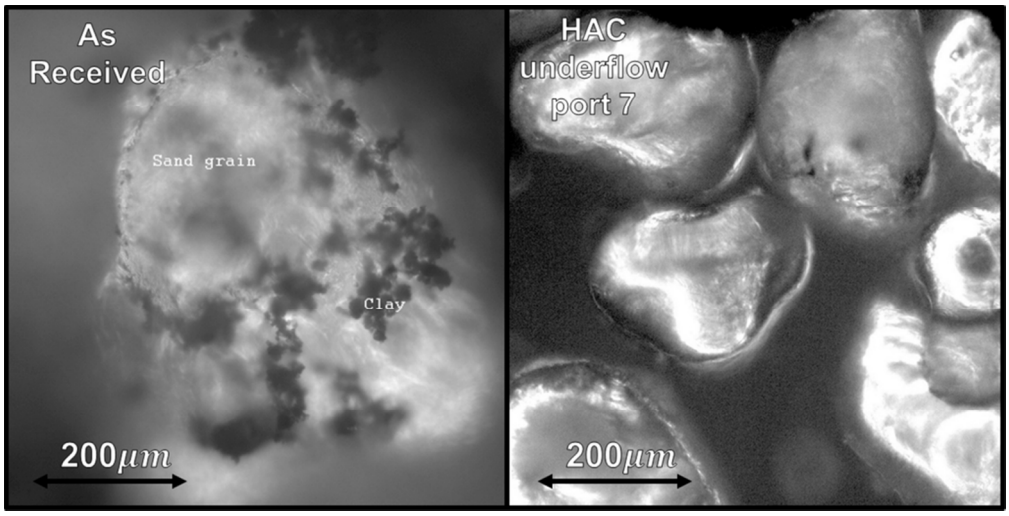

Figure 3

86x43mm (300 x 300 DPI)

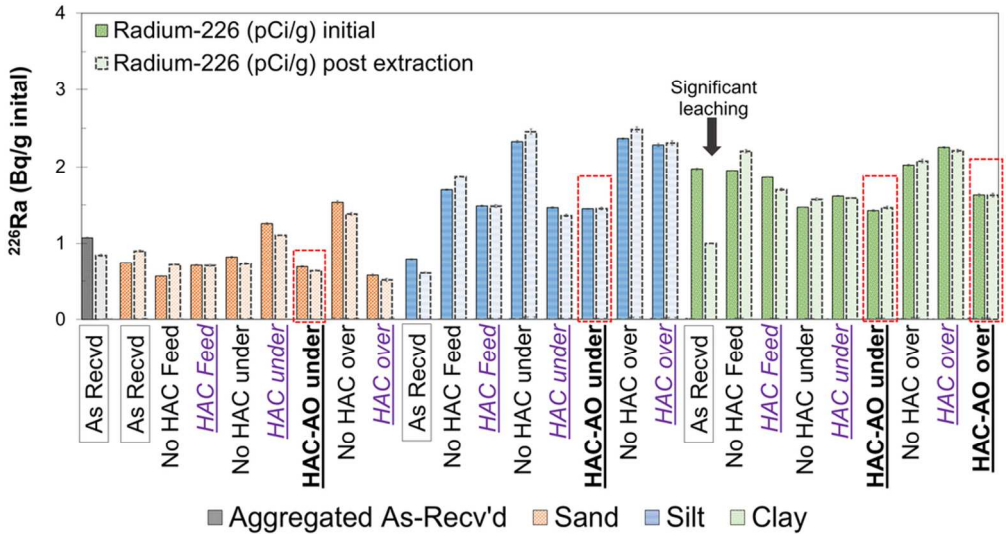

Figure 4

92x50mm (300 x 300 DPI)

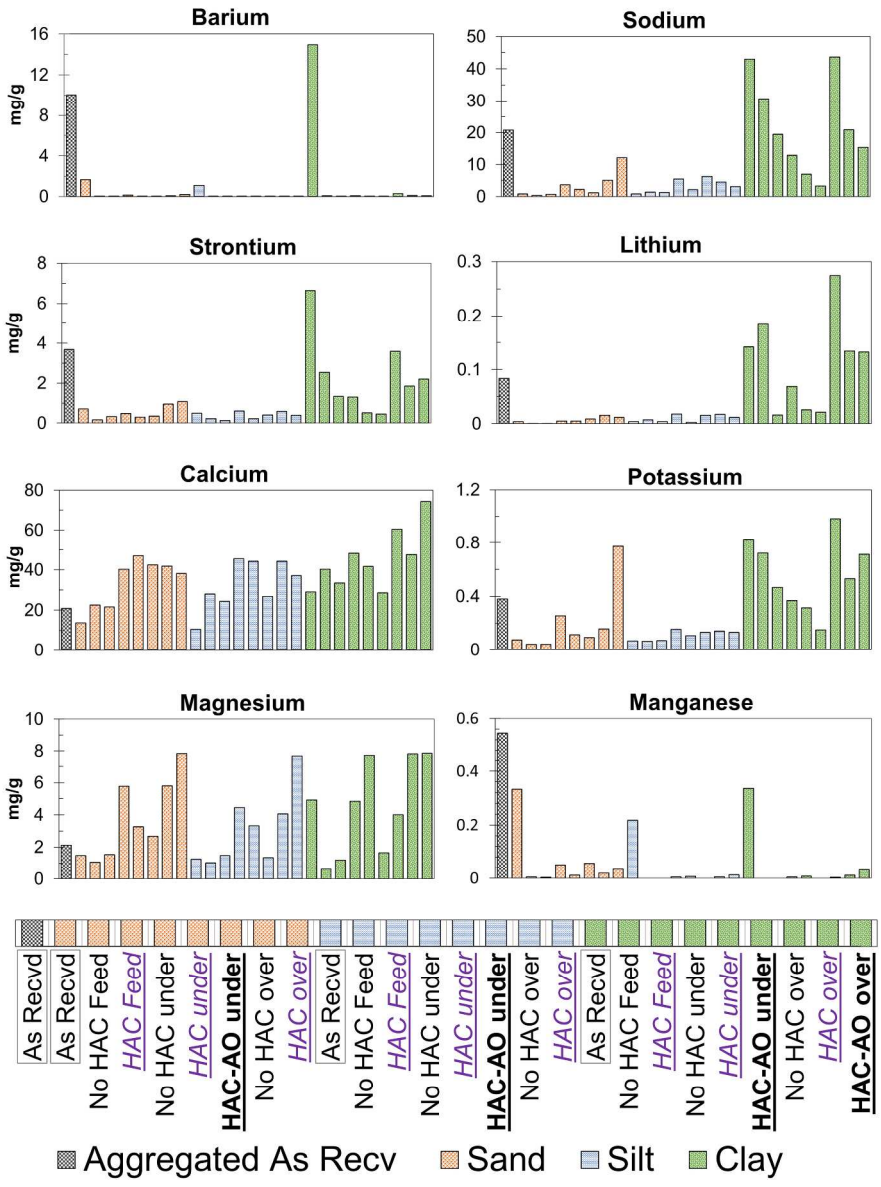

Figure 5

228x305mm (300 x 300 DPI)

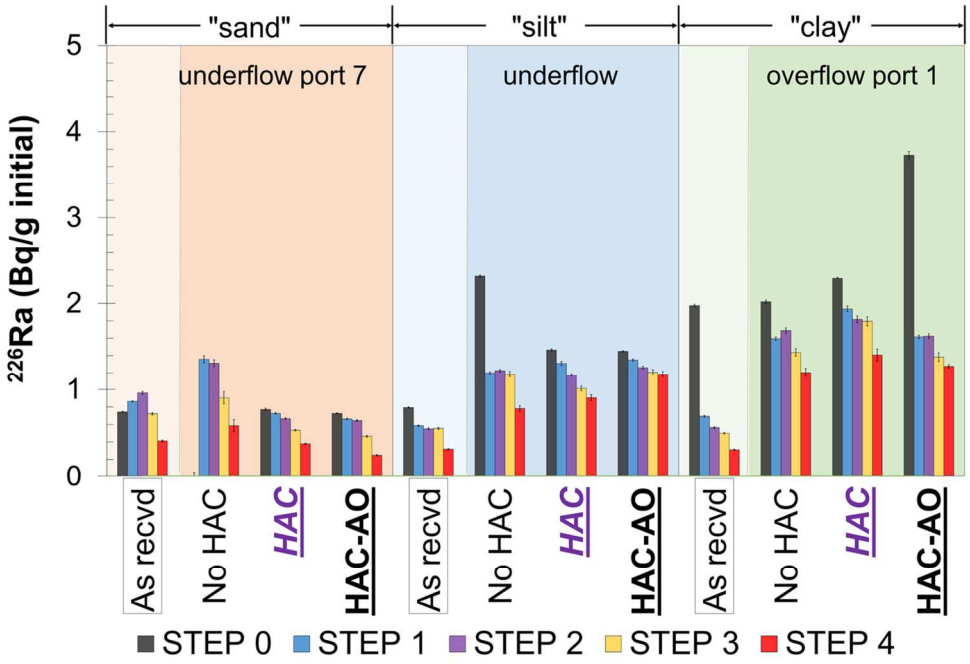

Figure 6

115x77mm (300 x 300 DPI)

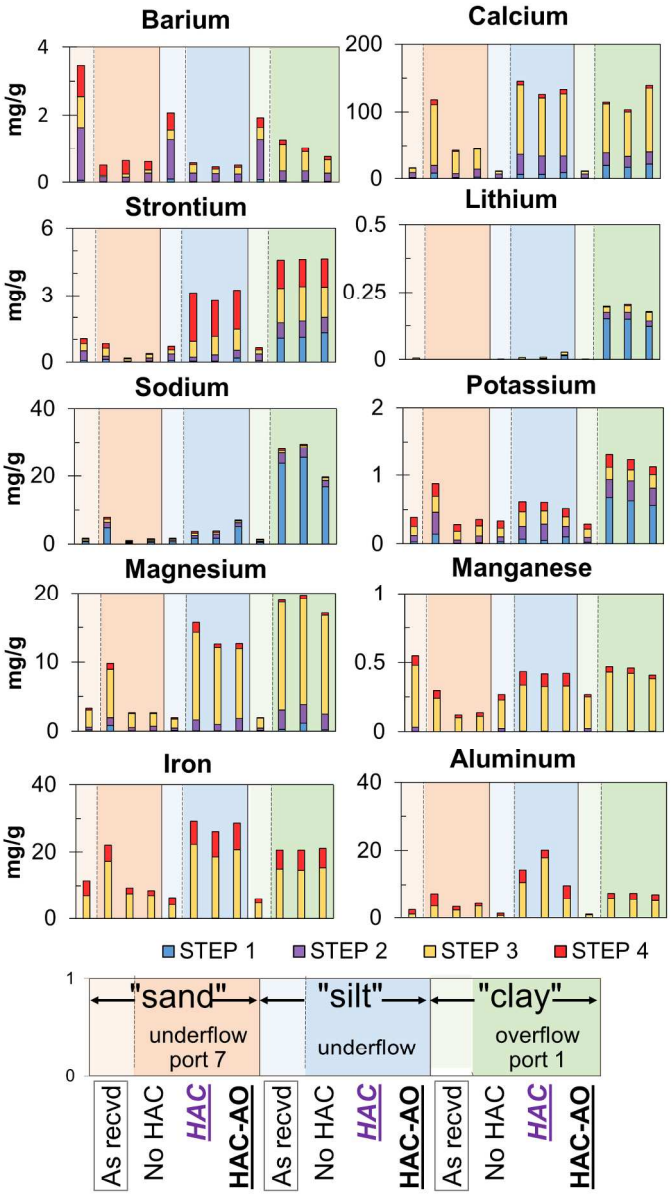

Figure 7

287x484mm (300 x 300 DPI)

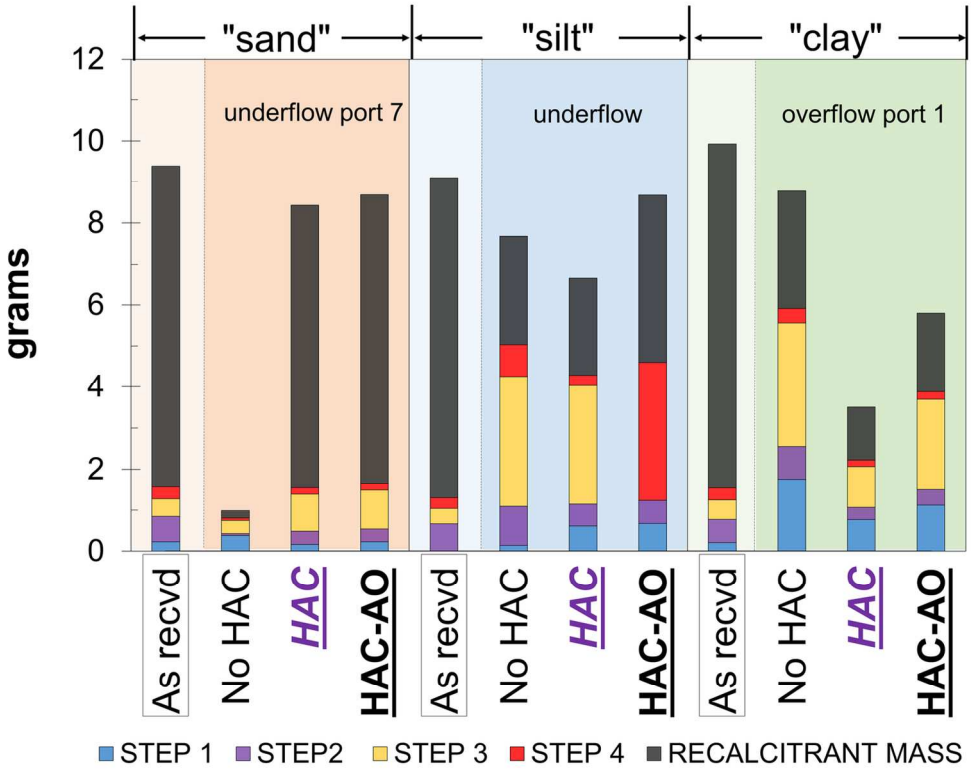

Figure 8

137x110mm (300 x 300 DPI)

Table 1. A four step sequential extraction was designed to investigate radium associations in the HAC-treated residual waste. After [73] and [74]. Extractions performed with 20:1 fluid-to-solid ratio. After extraction, solids were separated by centrifugation, rinsed with DI water, and dried. Radium-226 activities of the dried solids were determined by gamma spectroscopy.

Step	*Description*	*Extraction Targets*	*Target Examples*
0	Oven dried "As Recvd" and wet sieved, size-classified solids (includes TDS)	No extraction	All soluble and insoluble solids
1	Distilled-deionized (DI) Water for 24 hours	Soluble salts/evaporated pore water	NaCl, $BaCl_2$, $CaCl_2$, & $SrCl_2$
2	1M Ammonium Acetate for 12 hours	Surface exchangeable/ low-charge interlayer	From surface of sand and silt grains; from illite clay interlayer
3	9% Acetic Acid for 12 hours	Carbonate minerals	$CaCO_3$, $MgCO_3$, $Al_2(CO_3)_3$ & $Fe_2(CO_3)_3$
4	0.1 M Hydrochloric Acid for 12 hours	High-charge interlayer/partial silicate/oxides	MnO_x, FeO_x

Table 2. Summary of the mass-balance normalized raw material recovery for control (No HAC) and treatment (HAC). Up to 15% of the residual solid waste can be reclaimed as clays and 38% as sand.

Sampling point	*No HAC*		*HAC*	
	Clay	*Sand*	*Clay*	*Sand*
Feed	24%	35%	47%	23%
Overflow	8%	1%	11%	0%
Spiral Port 1	**8%**	1%	**10%**	0%
Spiral Port 2	**2%**	0%	**5%**	0%
Underflow	36%	7%	20%	14%
Spiral Port 3	5%	**1%**	2%	**3%**
Spiral Port 7	6%	**2%**	3%	**35%**

The percentage represents how much of the material sampled was clay (< 63 μm i.e. #230 mesh), or sand (>210 μm i.e #70 mesh), relative to the starting mass of the "As Received" material.

Table 3. Summary of the raw material recovery and market opportunity from HAC-treated residual waste assuming a disposal volume of 5,000 tons/y.

	Recovery	*Price of pristine material*	*Estimated benefit assuming 5,000 tons/y of residual solid*
Silica Sand	~37%	$84/ton [35]	Resell at $30/ton = $50,000 - $60,000/y
Resin coated/Ceramic proppant	~37%*	$200 - $500/ton [79]	Resell at $70 - $150/ton = $130,000 - $280,000/y
Wasted Material	~63%	**-$76/ton** [80]	Potential cost savings of $140,000/y

* Assuming similar recovery of resin coated sand or ceramic proppant as for silica sand.

PennState

Department of Civil and Environmental Engineering
College of Engineering
The Pennsylvania State University
212 Sackett Building
University Park, PA 16802-1408

814-863-3084
Fax: 814-863-7304
www.cee.psu.edu

By applying a novel system to unconventional oil and gas residual waste, we were able to recover valuable raw materials, which could represent significant savings to disposal cost, while aiding radioactivity management.

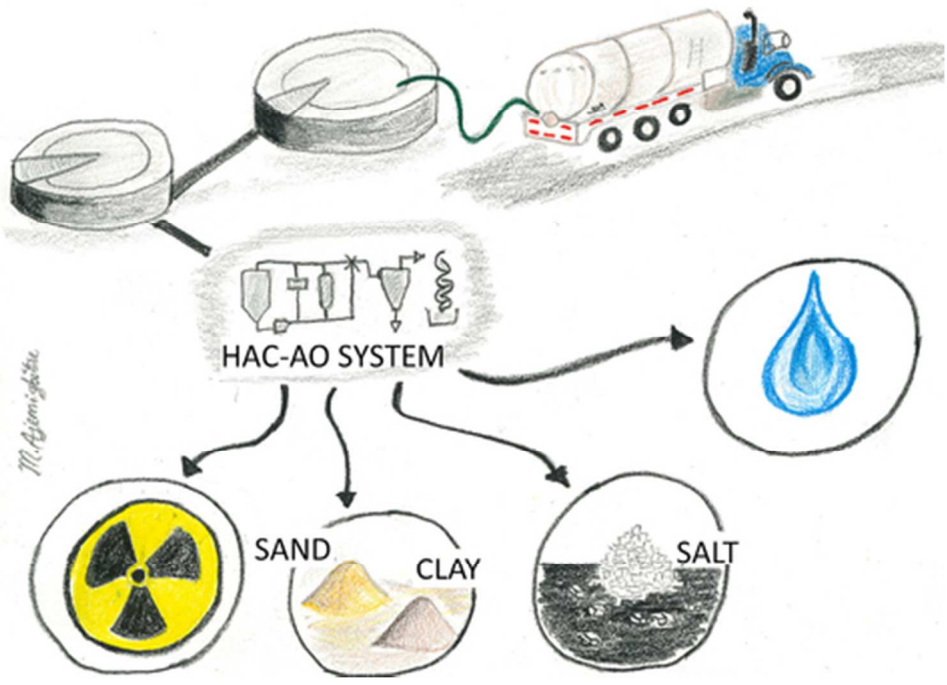

39x28mm (300 x 300 DPI)